

## Processable Cyclic Peptide Nanotubes with Tunable Interiors

Rami Hourani,<sup>†</sup> Chen Zhang,<sup>†</sup> Rob van der Weegen,<sup>‡</sup> Luis Ruiz,<sup>§</sup> Changyi Li,<sup>†</sup> Sinan Keten,<sup>§</sup> Brett A. Helms,<sup>\*,†</sup> and Ting Xu<sup>\*,†</sup>

<sup>†</sup>Department of Materials Science and Engineering, University of California, Berkeley, California 94720-1760, United States

<sup>‡</sup>The Molecular Foundry, Lawrence Berkeley National Laboratory, Berkeley, California 94720, United States

<sup>§</sup>Department of Civil & Environmental Engineering and Mechanical Engineering, Northwestern University, Evanston, Illinois 60208-3111, United States

**S** Supporting Information

**ABSTRACT:** A facile route to generate cyclic peptide nanotubes with tunable interiors is presented. By incorporating 3-amino-2-methylbenzoic acid in the D,L-alternating primary sequence of a cyclic peptide, a functional group can be presented in the interior of the nanotubes without compromising the formation of high aspect ratio nanotubes. The new design of such a cyclic peptide also enables one to modulate the nanotube growth process to be compatible with the polymer processing window without compromising the formation of high aspect ratio nanotubes, thus opening a viable approach toward molecularly defined porous membranes.

Organic nanotubes have unique advantages over carbon nanotubes and inorganic counterparts since their supramolecular assembly, often governed by secondary interactions, is fully reversible. They are useful building blocks to fabricate membranes for applications such as carbon capture, water desalination, and protective coatings.<sup>1–3</sup> There have been extensive efforts to design and synthesize nanotubes using dendrimers,<sup>4</sup> peptides,<sup>5</sup> peptidomimetics,<sup>6</sup> DNAs,<sup>7</sup> foldamers,<sup>8</sup> and J-type rosettes.<sup>9</sup> However, in order to fabricate technologically relevant membranes using organic nanotubes, there are two barriers: synthesizing nanotubes with a molecularly defined size, shape, and interior chemistry to control selectivity;<sup>10</sup> and modulating the nanotube assembly process to be compatible with polymers processing toward membrane fabrication.<sup>3</sup>

Cyclic peptides (CPs), comprised of an even number of alternating D- and L- $\alpha$ -amino acids, are particularly attractive since hydrogen bonding between adjacent cyclic peptides leads to stable 1-D hollow cyclic peptide nanotubes (CPNs) that exhibit transport properties similar to those seen in transmembrane proteins.<sup>11</sup> To further control mass transport through CPNs, attempts to modify their interiors have focused on incorporating artificial amino acids containing cyclohexanes and aromatic rings, or unsaturated amino acids at multiple positions in the canonical CP sequence to project a specific chemical functionality toward the pore interior.<sup>10,12,13</sup> Most of these approaches involve amino acid derivatives that are synthetically nontrivial, making it difficult to fabricate membranes at large scales. Synthesizing CPs using the solid phase peptide synthesis (SPPS) methodologies provides full control of the number and location of modifications in the peptide sequence.<sup>14</sup> These aspects of the synthesis are particularly

important to modify the exterior of CPNs for dispersion and directed nanotube growth in polymeric matrices. Also, the number and placement of noncanonical amino acids can have undesirable effects on the conformation of the ring and its potential for self-assembly. In many cases, the CP ring contorts owing to ring strain or otherwise rotates the backbone amide bonds. As a result, the efficacy of inter-ring hydrogen bonding is reduced and, in some cases, the formation of high aspect ratio CPNs is compromised.

Prototypical CPs have a strong tendency to form nanotube aggregates that are highly insoluble.<sup>15</sup> The solubility and the aspect ratio of CPNs can be tailored by attaching polymers to the exterior of nanotubes.<sup>16</sup> However, due to the obvious difficulties in vertically aligning 1-D nanotubes with a high aspect ratio in thin films, as is required for membrane fabrication, there is a need to modulate the assembly of CPN growth in a confined framework to macroscopically align nanotubes. There may also be additional opportunities to modulate the assembly through structural modifications to the primary sequence.<sup>3</sup>

We present here a minimalist approach that overcomes barriers to both generate peptide nanotubes with interior modification and dynamically tune the assembly process within the processing window of polymeric membranes. As an initial demonstration, a methyl group is introduced to the interior, although other functional groups might also be incorporated using orthogonal peptide chemistries and will be explored separately.<sup>17</sup> This was achieved by substituting one of the L-Leu in the primary sequence of a prototypical CP sequence *cyclo*-[L-Lys-D-Ala-L-Leu-D-Ala]<sub>2</sub> (8CP) using a single aromatic amino acid, 3-amino-2-methylbenzoic acid ( $\gamma$ -Mba-OH). The chemical structure of the Mba-modified cyclic peptide, *cyclo*-(L-Lys-D-Ala-L-Leu-D-Ala-L-Lys-D-Ala- $\gamma$ -Mba-D-Ala) (Mba-8CP, Figure 1a), is shown alongside the 8CP (Figure 1b) for comparison.

3-(9-Fluorenylmethoxycarbonyl)amino-2-methylbenzoic acid (Fmoc- $\gamma$ -Mba-OH) was prepared from 3-amino-2-methylbenzoic acid and N-(9-fluorenylmethoxycarbonyloxy) succinimide (Fmoc-OSu) in 80% yield. Both starting materials are commercially available, and the resulting Fmoc-protected amino acid can be made in large quantities and readily used in the SPPS. Mba-8CP and 8CP were synthesized on and cleaved from a 2-chlorotriptyl chloride resin prior to head-to-tail cyclization at

Received: July 7, 2011

Published: September 06, 2011

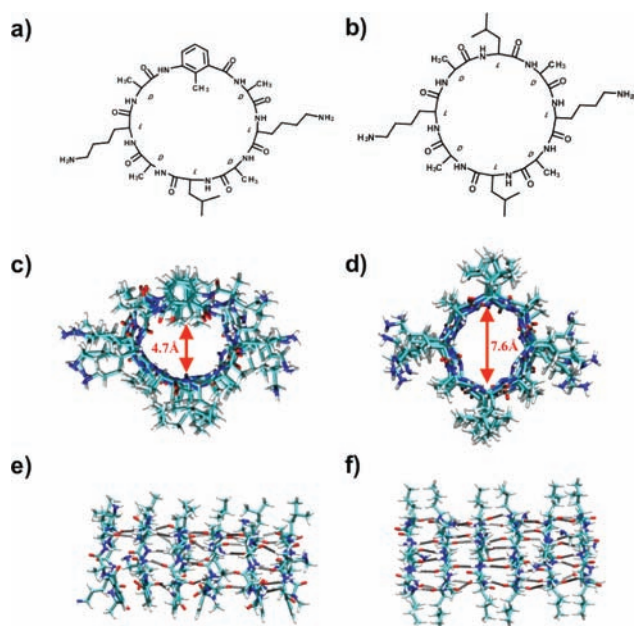


**Figure 1.** Chemical structures of (a) Mba-8CP and (b) its conventional analogue 8CP; Snapshots of equilibrium structures calculated from molecular dynamics (MD) simulations, showing cross-sectional (c,d) and lateral (e,f) views of Mba-8CP and 8CP nanotubes respectively. The internal diameters of Mba-8CP and 8CP are  $\sim 4.7$  and  $\sim 7.6$  Å, respectively, based on van der Waals radii.

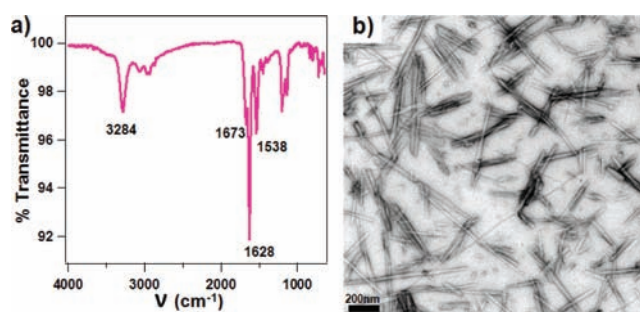


**Figure 2.** (a) FTIR spectrum of a thin film of Mba-8CP cast from ACN at room temperature. (b) TEM image of Mba-8CP nanotubes that aggregated into bundles, likely during the drying process. Scale bar: 200 nm.

high dilution in the presence of propane phosphonic acid anhydride (T3P) in 85% yield. After deprotection of the Boc groups on the lysine side chains, the crude materials were purified using preparative HPLC in an overall yield of 30%.

Molecular dynamics (MD) simulations were carried out to compare the structure and stability of the assemblies of Mba-8CP and 8CP. The simulations were performed using the COMPASS force field. Top views and side views of the equilibrated structures obtained from MD simulations are shown in Figure 1c–f. For Mba-8CP, the L-Leu to  $\gamma$ -Mba mutation points the methyl group into the interior of the pore as designed. This prominent hydrophobic group substantially reduces the internal diameter which is estimated to be  $\sim 4.7 \pm 0.6$  Å based on van der Waals radii (Figure 1c), a 38% reduction in size from the  $\sim 7.6$  Å pore size of the 8CP nanotube (Figure 1d). The aromatic rings of  $\gamma$ -Mba-OH are configured along one side of the nanotube, with slight tilts. The lateral views (Figure 1e,f) of the formed

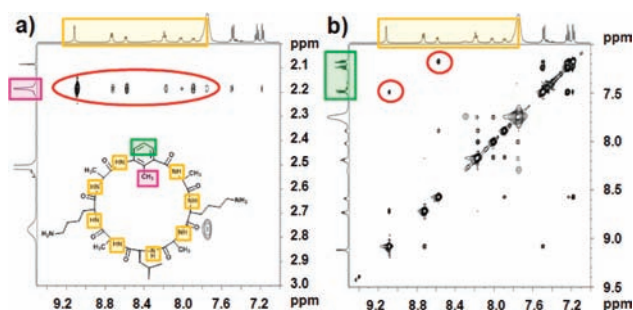


**Figure 3.** 2D NOESY spectra in  $d_6$ -DMSO of molecularly dissolved Mba-8CP indicating the through space correlations between the aromatic methyl group's protons in purple (a) and the aromatic protons in red (b) with the proton resonances of the amides in orange. The key cross-peaks are shown in red.

nanotubes showed that the mutation disproportionately elongates the ring structure and disrupts the symmetry of its amide bonds, and consequently the alignment of the carbonyl and amide groups in the antiparallel assembly. As a result, the number of hydrogen bonds between adjacent cyclic peptide rings is reduced from an average of 7.3 hydrogen bonds for 8CP to 5.9 for Mba-8CP. The average inter-ring distance is  $\sim 4.8$  Å in both cases (Figure S1).

Mba-8CP readily assembles into nanotubes in acetonitrile (ACN). Inter-ring hydrogen bonding for Mba-8CP was clearly observed at  $3284 \text{ cm}^{-1}$  using Fourier transform infrared (FTIR) spectroscopy (Figure 2a). Characteristic peaks for the amide Ia, amide Ib, and amide II regions at  $\nu$  1673, 1628, and  $1538 \text{ cm}^{-1}$  were consistent with those reported for 8CP.<sup>18</sup> Transmission electron microscopy (TEM) revealed bundles of nanotubes,  $\sim 100$ – $500$  nm in length (Figure 2b). The width of the bundles is between 20 and 40 nm, which corresponds to approximately over 20 individual Mba-8CPNs in a single aggregate. The dynamic light scattering (DLS) profile of Mba-8CP showed a nominal nanotube length of  $\sim 235$  nm, slightly smaller than that of  $\sim 377$  nm for 8CP (Figure S2).

Detailed spectroscopic characterizations using  $^1\text{H}$  and  $^1\text{H}$ - $^1\text{H}$ -COSY (Figure S3) NMR experiments were used to confirm the structure of Mba-8CP. A through-space 2D NOESY experiment was also carried out on a molecularly dissolved (i.e., disassembled) sample in DMSO to determine the orientation of the substituent at the 2-position of the aromatic amino acid in the modified CP (Figure S4). The methyl group of  $\gamma$ -Mba-OH at  $\delta$  2.19 ppm showed distinctive through-space interactions with each of the amide resonances in the CP backbone between 7.80 and 9.20 ppm (Figure 3a). This correlation was absent for the aromatic protons, except for the two neighboring amide protons on either side of the aromatic ring (Figure 3b). Similar studies were carried out in the ACN solution but were unsuccessful. The 2D NOESY results reflect the solution conformation of the Mba-8CP, which most likely represent the favorable conformation of the monomer in a CPN. This agrees well with the MD simulation that the methyl group was directed toward the inside of the CPN, while the aromatic protons were directed outward. Thus, by simply inserting this single aromatic amino acid into the primary sequence of the cyclic peptide 8-mer, its associated functional groups were presented in the interior of the nanotubes without compromising the formation of high aspect ratio assemblies.

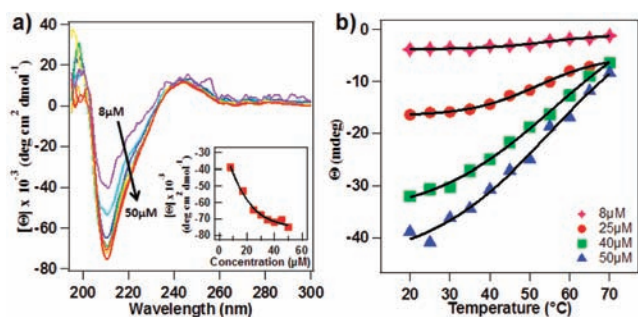


**Figure 4.** (a) CD spectra of Mba-8CP in ACN at different concentrations upon heating from 20 to 70 °C. The inset illustrates the dependence of molar ellipticity at 210 nm as a function of concentration. (b) The CD signal of Mba-8CP in ACN at 210 nm as a function of temperature for different concentrations. The heating rate is 5 °C/min with an equilibration time of 5 min.

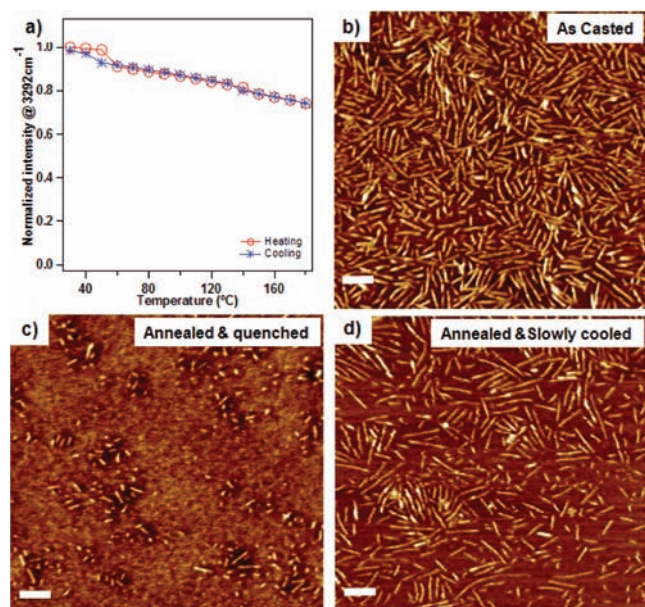


**Figure 5.** (a) Normalized absorptions of PEG-conjugated Mba-8CP for the heating and cooling cycles (30–180 °C) as a function of temperature using the intensity of the peak maximum at  $\nu = 3292 \text{ cm}^{-1}$  at 30 °C. AFM images of a spin-casted THF solution of PEG-conjugated Mba-8CP nanotubes (b), followed by solvent-annealing and quenching (c), followed by thermal annealing at 80 °C for 1 h and slow cooling (d) (Scale bar: 50 nm). Reversible growth of high aspect ratio PEG-covered CPNs of Mba-8CP can be clearly seen.

Theoretical calculations were also carried out to investigate the incorporation of two or more unnatural amino acids in the modified cyclic peptides. However, introduction of multiple modifications lead to either blocked pores or puckered cyclic peptide structures largely incapable of assembling into CPNs, as illustrated in Figure S5.

The mutation in the Mba-8CP sequence also suppressed to some extent the nanotube growth. The solution phase assembly of Mba-8CP was studied as a function of concentration and temperature using circular dichroism (CD) spectroscopy. CPNs from Mba-8CP in ACN showed a distinctive negative Cotton effect at  $\lambda = 210 \text{ nm}$  (Figure 4a). Increasing the concentration of Mba-8CP increased the intensity of the CD signal at 210 nm,

toward a plateau at  $\sim 40 \mu\text{M}$ . The dissociation constant  $K_d$  was found to be  $21 \pm 5 \mu\text{M}$ . The assembly process of Mba-8CP was determined to be completely thermoreversible within the experimental conditions applied. Figure 4b relates the magnitude of the Cotton effect at 210 nm for Mba-CP derived nanotubes in ACN at different concentrations upon heating from 20 to 70 °C. The effect of temperature on the CD signal profile was dependent on the concentration of the Mba-8CP. As the temperature is increased, the CD signals of all profiles approach a similar equilibrium state closer to the molecularly dissolved state. Similar studies with the regular 8CP could not be achieved due to its lower solubility and much stronger hydrogen bonding among the rings, which showed little thermal losses in the CD signal. The dependence of the reversible assembly process on concentration and temperature in the case of CPNs derived from Mba-8CP points to distinct opportunities to process smooth polymer thin films from solution.

To ensure the reversible assembly process of Mba-8CP does not compromise the formation of high aspect ratio CPNs, we monitored the nanotube growth using polyethylene glycol (PEG)-covered CPNs of Mba-8CP. HO-PEG-NHCOCH<sub>2</sub>CH<sub>2</sub>COOH ( $M_w = 3000 \text{ g/mol}$ ) was conjugated to Mba-8CP by coupling to the amino groups of lysine residues of Mba-8CP as described previously.<sup>3</sup> The nanotube growth process of PEG-conjugated Mba-8CP in the solid state was studied *in situ* using FTIR spectroscopy by monitoring the N–H stretching vibration at  $3292 \text{ cm}^{-1}$  upon heating from 30 to 180 °C. The nanotubes reformed upon cooling with only a slight hysteresis (Figure 5a). Upon spin-casting onto a silicon substrate with a native silicon oxide layer, the PEG-conjugated Mba-8CPNs that are 50–150 nm in length can be easily visualized (Figure 5b). The width of the formed nanotube is  $\sim 5.5 \text{ nm}$  (the height is  $\sim 0.5 \text{ nm}$ ), which corresponds to individual PEG-covered Mba-8CPNs.<sup>16</sup> This confirms the advantage of attaching polymers to CPNs in reducing their tendency to aggregate, hence rendering them more processable. The assembly of the casted CPNs can be readily disrupted by thermal or solvent annealing; typical treatments to prepare polymeric membranes (Figure 5c). The high aspect ratio nanotubes reform upon thermal annealing followed by slow cooling (Figure 5d).

Since the assembly of cyclic peptides is a highly directional 1-D growth process and the overall properties of nanotubes are influenced by the molecular scale building blocks, we see a viable path toward organic nanotubes with molecularly defined interiors to mimic transmembrane proteins for enhanced selectivity in molecular recognition, transport, and separation processes. The added advantage of this new design is the ability to manipulate the nanotube formation to be compatible with the processing window of polymeric membranes so that subunits or short nanotubes, rather than high aspect ratio nanotubes, can be incorporated into a polymer matrix and, subsequently, grow nanotubes *in situ* to fabricate functional membranes.

## ■ ASSOCIATED CONTENT

**S Supporting Information.** Experimental and computational details and characterization of materials synthesized. This material is available free of charge via the Internet at <http://pubs.acs.org>.

## ■ AUTHOR INFORMATION

### Corresponding Author

bahelms@lbl.gov; tingxu@berkeley.edu

## ACKNOWLEDGMENT

We acknowledge support from the DOE-EFRC for Gas Separations Relevant to Clean Energy Technologies under Award Number DE-SC0001015 (R.H., C.Z., B.H., T.X.); Army Research Office under Contract No. W91NF-09-1-0374 (R.vdW., C.L., T.X.). R.H. thanks FQRNT (Québec, Canada) for a postdoctoral fellowship. S.K. and L.R. acknowledge a super-computing grant from Northwestern University Quest HPC system and support from CEE & ME departments. Portions of this work (e.g., synthesis of  $\gamma$ -Mba-OH, CPs, and spectroscopic characterization) were performed as a User project at the Molecular Foundry, funded by the DOE under Contract No. DE-AC02-05CH11231. We thank H. Dong for the TEM measurements and J. Pelton for help and discussions about the NMR studies.

## REFERENCES

- (1) (a) Gin, D. L.; Noble, R. D. *Science* **2011**, *332*, 674–676. (b) Kaucher, M. S.; Peterca, M.; Dulcey, A. E.; Kim, A. J.; Vinogradov, S. A.; Hammer, D. A.; Heiney, P. A.; Percec, V. *J. Am. Chem. Soc.* **2007**, *129*, 11698–11699.
- (2) Shannon, M. A.; Bohn, P. W.; Elimelech, M.; Georgiadis, J. G.; Marinas, B. J.; Mayes, A. M. *Nature* **2008**, *452*, 301–310.
- (3) Xu, T. Z.; Ren, F.; Hourani, R.; Lee, M. T.; Shu, J. Y.; Mao, S.; Helms, B. A. *ACS Nano* **2011**, *5*, 1376–1384.
- (4) Percec, V.; Dulcey, A. E.; Balagurusamy, V. S. K.; Miura, Y.; Smidrkal, J.; Peterca, M.; Nummelin, S.; Edlund, U.; Hudson, S. D.; Heiney, P. A.; Hu, D. A.; Magonov, S. N.; Vinogradov, S. A. *Nature* **2004**, *430*, 764–768.
- (5) Kholkin, A.; Amdursky, N.; Bdikin, I.; Gazit, E.; Rosenman, G. *ACS Nano* **2010**, *4*, 610–614.
- (6) Hartgerink, J. D.; Granja, J. R.; Milligan, R. A.; Ghadiri, M. R. *J. Am. Chem. Soc.* **1996**, *118*, 43–50.
- (7) Davis, J. T.; Spada, G. P. *Chem. Soc. Rev.* **2007**, *36*, 296–313.
- (8) Zang, L.; Che, Y.; Moore, J. S. *Acc. Chem. Res.* **2008**, *41*, 1596–1608.
- (9) Sakai, N.; Kamikawa, Y.; Nishii, M.; Matsuoka, T.; Kato, T.; Matile, S. *J. Am. Chem. Soc.* **2006**, *128*, 2218–2219.
- (10) (a) Amorin, M.; Castedo, L.; Granja, J. R. *J. Am. Chem. Soc.* **2003**, *125*, 2844–2845. (b) Reiriz, C.; Brea, R. J.; Arranz, R.; Carrascosa, J. L.; Garibotti, A.; Manning, B.; Valpuesta, J. M.; Eritja, R.; Castedo, L.; Granja, J. R. *J. Am. Chem. Soc.* **2009**, *131*, 11335–11337. (c) Horne, W. S.; Stout, C. D.; Ghadiri, M. R. *J. Am. Chem. Soc.* **2003**, *125*, 9372–9376. (d) Reiriz, C.; Amorin, M.; García-Fandiño, R.; Castedo, L.; Granja, J. R. *Org. Biomol. Chem.* **2009**, *7*, 4358–4361.
- (11) (a) Ghadiri, M. R.; Granja, J. R.; Buehler, L. K. *Nature* **1994**, *369*, 301–304. (b) Brea, R. J.; Reiriz, C.; Granja, J. R. *Chem. Soc. Rev.* **2010**, *39*, 1448–1456.
- (12) (a) Kubik, S.; Goddard, R. *J. Org. Chem.* **1999**, *64*, 9475–9486. (b) Kubik, S. *J. Am. Chem. Soc.* **1999**, *121*, 5846–5855. (c) Ishida, H.; Qi, Z.; Sokabe, M.; Donowaki, K.; Inoue, Y. *J. Org. Chem.* **2001**, *66*, 2978–2989. (d) Kubik, S.; Goddard, R. *Chem. Commun.* **2000**, 633–634. (e) Kubik, S. *Chem. Soc. Rev.* **2009**, *38*, 585–605. (f) Gauthier, D.; Baillargeon, P.; Drouin, M.; Dory, Y. L. *Angew. Chem., Int. Ed.* **2001**, *40*, 4635–4638. (g) Leclair, S.; Baillargeon, P.; Skouta, R.; Gauthier, D.; Zhao, Y.; Dory, Y. L. *Angew. Chem., Int. Ed.* **2004**, *43*, 349–353.
- (13) (a) Amorin, M.; Castedo, L.; Granja, J. R. *Chem.—Eur. J.* **2005**, *11*, 6543–6551. (b) Amorin, M.; Villaverde, V.; Castedo, L.; Granja, J. R. *J. Drug Delivery Sci. Technol.* **2005**, *15*, 87–93. (c) Brea, R. J.; Castedo, L.; Granja, J. R. *Chem. Commun.* **2007**, 3267–3269. (d) Brea, R. J.; Amorin, M.; Castedo, L.; Granja, J. R. *Angew. Chem., Int. Ed.* **2005**, *44*, 5710–5713. (e) Amorin, M.; Brea, R. J.; Castedo, L.; Granja, J. R. *Org. Lett.* **2005**, *7*, 4681–4684. (f) Amorin, M.; Castedo, L.; Granja, J. R. *Chem.—Eur. J.* **2008**, *14*, 2100–2111.
- (14) Atherton, E.; Sheppard, R. C. *Solid Phase Peptide Synthesis: A Practical Approach*; Oxford University Press; USA, 1989.
- (15) (a) Khazanovich, N.; Granja, J. R.; McRee, D. E.; Milligan, R. A.; Ghadiri, M. R. *J. Am. Chem. Soc.* **1994**, *116*, 6011–6012. (b) Ghadiri, M. R.; Kobayashi, K.; Granja, J. R.; Chadha, R. K.; McRee, D. E. *Angew. Chem., Int. Ed. Engl.* **1995**, *34*, 93–95. (c) Kobayashi, K.; Granja, J. R.; Ghadiri, M. R. *Angew. Chem., Int. Ed. Engl.* **1995**, *34*, 95–98. (d) Clark, T. D.; Ghadiri, M. R. *J. Am. Chem. Soc.* **1995**, *117*, 12364–12365. (e) Ghadiri, M. R.; Granja, J. R.; Milligan, R. A.; McRee, D. E.; Khazanovich, N. *Nature* **1993**, *366*, 324–327.
- (16) (a) ten Cate, M. G. J.; Severin, N.; Borner, H. G. *Macromolecules* **2006**, *39*, 7831–7838. (b) Couet, J.; Biesalski, M. *Small* **2008**, *4*, 1008–1016. (c) Couet, J.; Jayaprakash, J. D.; Samuel, S.; Kopyshv, A.; Santer, S.; Biesalski, M. *Angew. Chem., Int. Ed.* **2005**, *44*, 3297–3301.
- (17) (a) Hermanson, G. T. *Bioconjugate Techniques*; Academic Press, Elsevier Inc.: London, U.K., 2008. (b) Chan, C. W.; White, P. D. *Fmoc solid phase peptide synthesis: A practical approach*; Oxford University Press: New York, USA, 2000.
- (18) (a) Krimm, S.; Bandekar, J. In *Advances in Protein Chemistry*; Anfinsen, C. B., Edsall, J. T., Richards, F. M., Eds.; Academic Press: Orlando, FL, 1986; pp 181–364. (b) Haris, P. I.; Chapman, D. *Biopolymers (Peptide Sci.)* **1995**, *37*, 251–263. (c) Clark, T. D.; Buehler, L. K.; Ghadiri, M. R. *J. Am. Chem. Soc.* **1998**, *120*, 651–656.